Received: 10 October 2022 | Revised: 7 April 2023 | Accepted: 13 April 2023

DOI: 10.1002/jsp2.1257

RESEARCH ARTICLE

JOR Spine OPEN ACCESS

In vitro coupled motions of the whole human thoracic and lumbar spine with rib cage

Mattan R. Orbach[1] | Jonathan Mahoney[2] | Brandon S. Bucklen[2] | Sriram Balasubramanian[1]

[1]School of Biomedical Engineering, Science and Health Systems, Drexel University, Philadelphia, Pennsylvania, USA

[2]Musculoskeletal Education and Research Center, A Division of Globus Medical, Inc, Audubon, Pennsylvania, USA

Correspondence
Sriram Balasubramanian, School of Biomedical Engineering, Science and Health Systems, Drexel University, 3141 Chestnut St, Bossone 718, Philadelphia, PA, 19104 USA.
Email: sri.bala@drexel.edu

Abstract

Study design: In vitro biomechanical study investigating the coupled motions of the whole normative human thoracic spine (TS) and lumbar spine (LS) with rib cage.

Objective: To quantify the region-specific coupled motion patterns and magnitudes of the TS, thoracolumbar junction (TLJ), and LS simultaneously.

Background: Studying spinal coupled motions is important in understanding the development of complex spinal deformities and providing data for validating computational models. However, coupled motion patterns reported in vitro are controversial, and no quantitative data on region-specific coupled motions of the whole human TS and LS are available.

Methods: Pure, unconstrained bending moments of 8 Nm were applied to seven fresh-frozen human cadaveric TS and LS specimens (mean age: 70.3 ± 11.3 years) with rib cages to elicit flexion-extension (FE), lateral bending (LB), and axial rotation (AR). During each primary motion, region-specific rotational range of motion (ROM) data were captured.

Results: No statistically significant, consistent coupled motion patterns were observed during primary FE. During primary LB, there was significant ($p < 0.05$) ipsilateral AR in the TS and a general pattern of contralateral coupled AR in the TLJ and LS. There was also a tendency for the TS to extend and the LS to flex. During primary AR, significant coupled LB was ipsilateral in the TS and contralateral in both the TLJ and LS. Significant coupled flexion in the LS was also observed. Coupled LB and AR ROMs were not significantly different between the TS and LS or from one another.

Conclusions: The findings support evidence of consistent coupled motion patterns of the TS and LS during LB and AR. These novel data may serve as reference for computational model validations and future in vitro studies investigating spinal deformities and implants.

KEYWORDS

axial rotation, biomechanics, coupled motion, extension, flexion, in vitro, kinematics, lateral bending, lumbar spine, range of motion, thoracic spine, thoracolumbar junction

1 | INTRODUCTION

Studies have reported evidence of spinal coupled motions for over a century. As early as 1905, a landmark spinal kinematics study by Lovett[1] qualitatively demonstrated mechanical coupled motions of the human spine in both cadaveric specimens and living subjects. Coupled motions are defined as secondary movements that consistently accompany a primary motion. The two spinal motions most prominently reported to be coupled are lateral bending (LB) and axial rotation (AR). Studying this coupled motion behavior in the whole thoracic spine (TS) and lumbar spine (LS) is especially of interest, as it may aid in better understanding the development of scoliosis.[1–4] Specifically, the natural coupled motions of the spine are thought to remain present in and contribute to the formation of scoliotic deformities, as there is a correlation between the magnitudes of coronal curvature and accompanying AR in the scoliotic spine.[4] The study of spinal coupled motions is also thought to have clinical utility in the diagnosis of spinal instability due to trauma or degeneration.[5] Furthermore, abnormalities in coupled motions have been previously reported in patients suffering from back pain.[6,7] However, to identify abnormal patterns, it is important to first quantify normal coupled motions.

Despite how long spinal coupled motions have been a topic of study, the contributing factors are still not well understood. Thus, in addition to developing mathematical models,[8,9] in vitro studies are performed to understand the sole influence of structural and osteoligamentous factors as well as sagittal posture on coupled motion patterns without considering the effects of the neuromuscular system. Such in vitro studies have discovered that the complex anatomical shapes of functional spinal units (FSUs)—especially the multiplanar facet joint orientations, including the sagittal angles that they form—contribute to spinal coupled motions.[10] Although there is a consensus about in vitro coupled motion patterns of the LS,[11-13] controversy still exists about such patterns of the TS[10,14,15] despite the more controlled in vitro test conditions. Furthermore, previous in vitro studies have analyzed coupled motion patterns of only the TS,[10,16] thoracolumbar junction (TLJ),[17] or LS.[11-13] To the authors' knowledge, no quantitative data exist on in vitro region-specific coupled motions of the whole human TS and LS (T1–L5) with rib cage. Such kinematics data may be used to validate computational models of the spine[18-20] that predict the performance of implants and surgical interventions, and to better understand spinal biomechanics in deformity,[21-23] degeneration, and trauma[24-28] as well as the biofidelity of surrogate animal spine models.[29]

Therefore, the objective of this in vitro biomechanical study is to quantify the coupled motions of the whole human TS and LS with rib cage. Such data will help better understand the regional differences in spinal coupled motion patterns and magnitudes.

2 | MATERIALS AND METHODS

2.1 | Specimen preparation

Seven fresh-frozen human cadaveric TS and LS (T1–L5) specimens with rib cage (mean age: 70.3 ± 11.3 years, mean *T*-score: −2.4 ± 1.1) underwent range of motion (ROM) testing. However, one specimen did not include vertebral levels T1–T2 and another did not include T1–T3 (Table 1). Since testing involved applying an unconstrained, pure moment that is presumed to be uniform in magnitude at every level of the spine,[30] regardless of the number of involved FSUs, all specimens were included in this study. Upon radiographic screening, no specimens exhibited signs of trauma, fractures, malignancy, or deformity (e.g., collapsed discs, osteophytes, or facet joint hypertrophy) that would otherwise affect spinal kinematics.

During dissection, the surrounding musculature was carefully removed while the pertinent intervertebral discs, osteoligamentous structures, and joint capsules were preserved. Afterward, the cranialmost and L5 vertebrae were potted parallel to their endplates using a 1:1 mixture of Bondo body filler and fiberglass resin (Bondo Mar-Hyde Corp.). Before potting, screws were inserted into these vertebrae to improve fixation inside the mixture. For some specimens, resection of a portion of the most cephalad rib necks was required so that the corresponding, uppermost vertebrae could be adequately potted. Since the initial sagittal posture affects the pattern and magnitude of observed coupled motions of the TS[31] and LS,[13] thoracic kyphosis (T5–T12) and lumbar lordosis (L1–L5) were measured using the modified Cobb method to assess the neutral posture of each specimen in the upright position. These sagittal angles, as well as the demographic and anthropometric measurements for each specimen, are provided in Table 1.

2.2 | Motion data collection

After being thawed overnight at room temperature, each specimen was mounted on a custom six-degrees-of-freedom (6DOF) spine motion simulator at the potted superior and inferior vertebral ends for ROM testing. Utilizing three servoelectric motors and near-frictionless air bearings, the 6DOF spine motion simulator applied pure, unconstrained bending moments of ±8 Nm, which is within the range of previously reported values,[15,17,32-34] at an angular displacement rate of 1 °/s[35] along each cardinal plane to elicit flexion-extension (FE), LB, and AR motions. For each primary motion, the first two loading/unloading cycles were performed to precondition and account for viscoelastic effects, and the third cycle was considered for analysis.[33] All specimens were kept hydrated using saline solution (0.9%) throughout testing to retain viscoelastic properties.

To capture the region-specific motion data from each specimen using the motion analysis system (Optotrak Certus®; Northern Digital, Inc.), markers (each containing three infrared light-emitting diodes) were rigidly affixed to the superior and inferior pots of T1 and L5, as well as to the T12 and L1 vertebrae, using bone screws (Figure 1). The Optotrak Certus® system superimposes the coordinate systems of two markers (i.e., vertebral bodies) to yield relative Eulerian rotation angles in each of the three planes of motion at a data sampling frequency of 100 Hz. The system's reported resolution, and rotation and translational accuracies, are 0.01 mm,[36] 0.05°, and 0.03 mm,[37] respectively.

TABLE 1 Demographic and anthropometric values of each specimen and the vertebral levels each specimen is comprised of. Thoracic kyphosis and lumbar lordosis angles are also provided.

Specimen no.	Age (years)	Sex	Height (cm)	BMI (kg/m^2)	Vertebral levels	Thoracic kyphosis (°)	Lumbar lordosis (°)
1	87	Female	160.0	20.4	T1–L5	30.1	24.3
2	64	Male	167.6	16.2	T1–L5	40.7	21.2
3	79	Female	167.6	35.6	T1–L5	25.9	27.2
4	80	Female	165.1	25.0	T3–L5	32.0	26.7
5	62	Female	175.3	37.0	T4–L5	15.6	19.4
6	61	Male	175.3	15.7	T1–L5	41.8	25.5
7	59	Female	172.7	27.4	T1–L5	38.8	26.1

Abbreviation: BMI, body mass index.

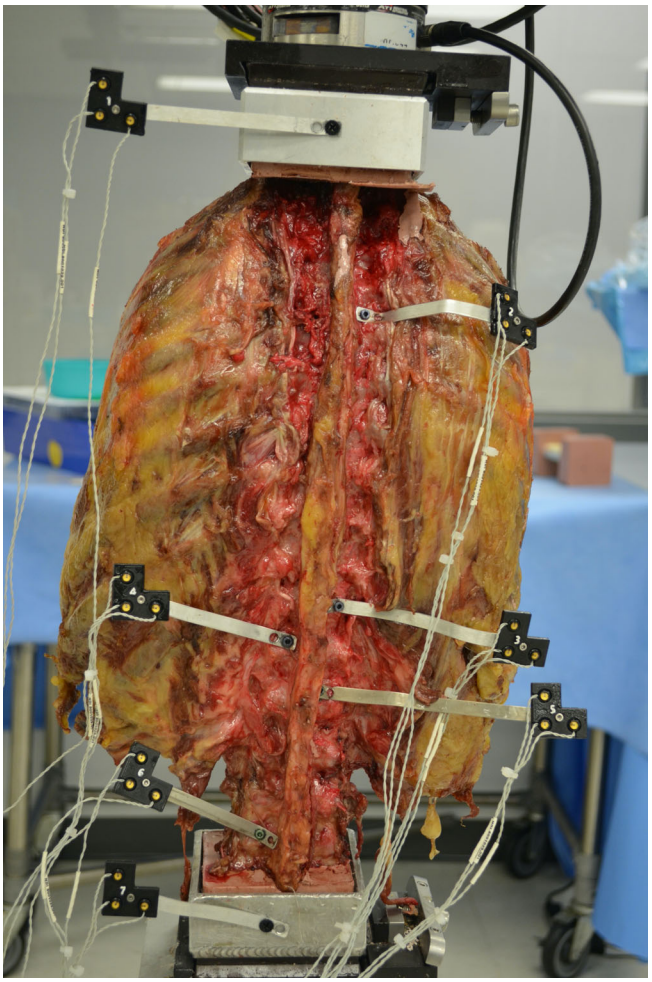

FIGURE 1 Range of motion (ROM) test setup for whole thoracic and lumbar spine specimen 3. The specimen is mounted to a custom six-degrees-of-freedom (6DOF) spine motion simulator at the potted T1 and L5 vertebral levels. Markers pertinent to this study were affixed at T1 (potted), T12, L1, and L5 (potted) vertebral levels to collect region-specific rotational range of motion data using the Optotrak Certus® motion analysis system (Northern Digital Inc.).

2.3 | Data analysis

From the collected relative rotational motion data, the ranges of both the primary and coupled motions occurring in the TS (T1–T12), TLJ (T12–L1), and LS (L1–L5) were calculated and plotted using MATLAB R2018b (The MathWorks, Inc.). Each range of coupled motion was then expressed as a percentage of the range of the respective primary motion, and the Shapiro–Wilk test was performed to check for normality. After determining that the data followed non-normal distributions, Wilcoxon signed-rank tests were performed to identify statistically significant coupled motions occurring during the positive and negative directions of primary motion. All statistics were calculated using SPSS v16.0 (IBM Corp.), with a p value of <0.05 considered statistically significant.

3 | RESULTS

Bar plots summarizing the median values and interquartile ranges (Table A1) of the primary and coupled motions of the TS, TLJ, and LS are provided in Figure 2. Only TLJ and LS kinematic data were collected from specimens 4 and 5 as they were potted below T1. Exemplar moment-angular displacement curves of whole TS and LS (T1–L5) coupled motions occurring during each primary motion over the duration of the third loading/unloading cycle are shown in Figure 3. On average, the contributions of the TS, TLJ, and LS to the overall primary flexion ROM of the whole spine were 59.2%, 5.9%, and 34.8%, respectively. No statistically significant coupled motions were observed during primary flexion. The average contributions of the TS, TLJ, and LS to the overall primary extension ROM were 66.1%, 3.4%, and 30.5%, respectively. During primary extension, unexpected statistically significant ($p < 0.05$) coupled right LB and AR occurred in the TLJ and LS, respectively.

On average, the contributions of the TS, TLJ, and LS to the overall primary LB ROM of the whole spine were 60.2%, 3.6%, and 36.2%, respectively. The only statistically significant ($p < 0.05$) coupled motion that occurred during primary LB was ipsilateral AR in the TS. However, a general trend of contralateral coupled AR in the TLJ and LS was observed. Additionally, there were general tendencies for the TS to extend and the LS to flex.

On average, the contributions of the TS, TLJ, and LS to the overall primary AR ROM of the whole spine were 69.3%, 4.5%, and 26.2%, respectively. Statistically significant ($p < 0.05$) coupled LB patterns occurred in all three regions during primary AR; the coupled LB was in the ipsilateral direction in the TS and in the contralateral direction in both the TLJ and LS. There was also statistically significant ($p < 0.05$) coupled FE in the TLJ, but in no specific direction. There was no generally

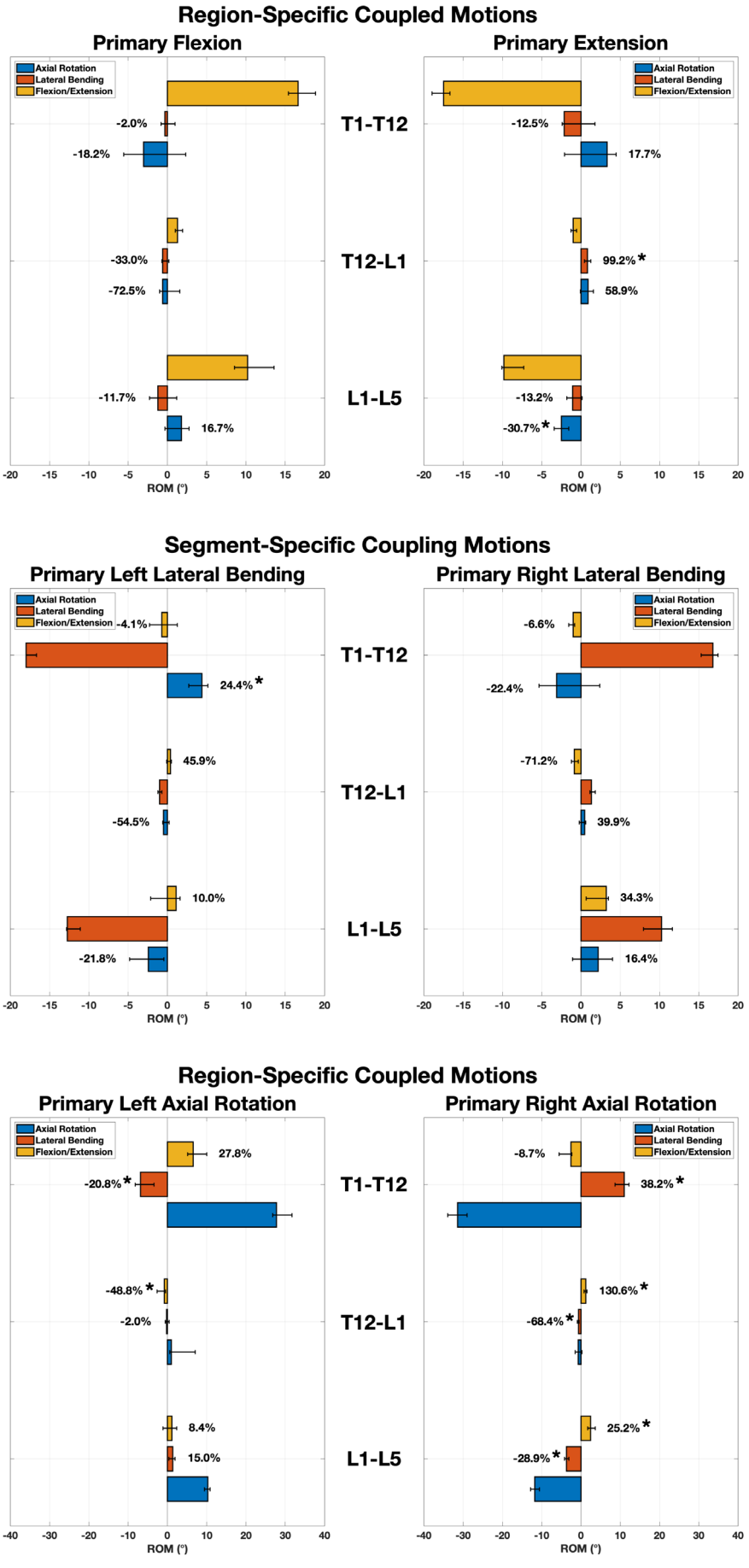

FIGURE 2 Median values and interquartile ranges (represented by the error bars) of thoracic (T1–T12, $n = 5$), thoracolumbar junction (T12–L1, $n = 7$), and lumbar (L1–L5, $n = 7$) coupled motions during the positive and negative directions of each primary motion. Flexion, right lateral bending, and left axial rotation are in the positive direction. Extension, left lateral bending, and right axial rotation are in the negative direction. Median values of the coupled motions expressed as percentages of their respective primary motion magnitudes are also provided. $^{*}p < 0.05$.

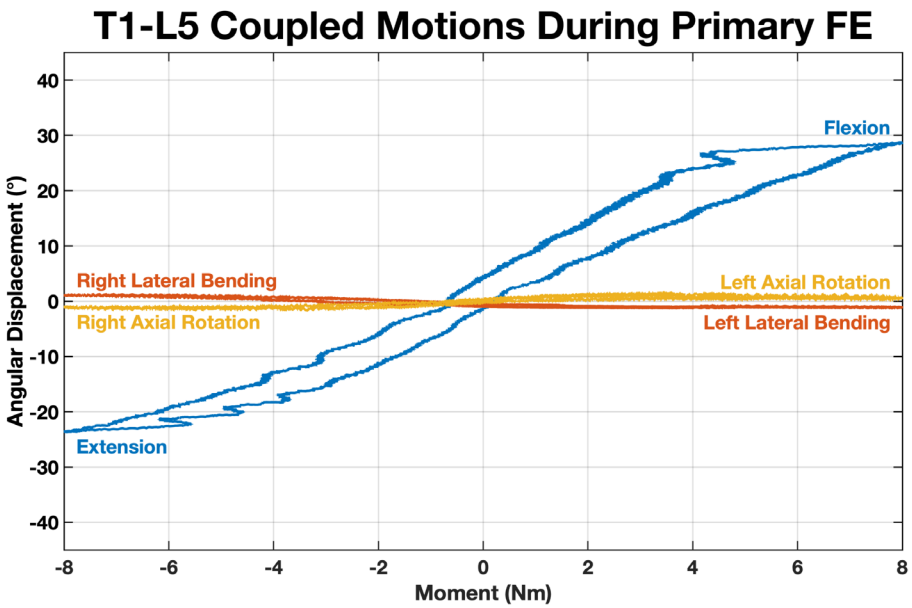

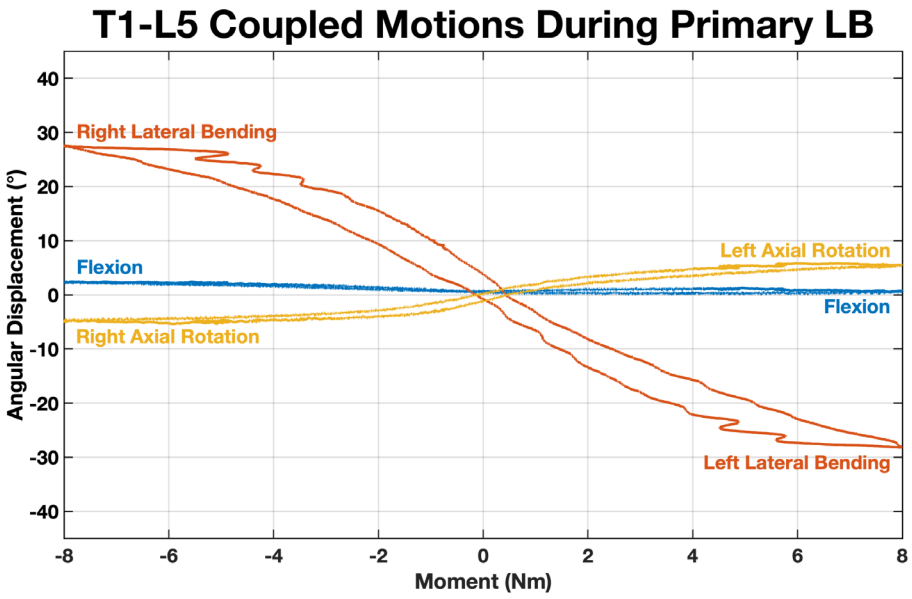

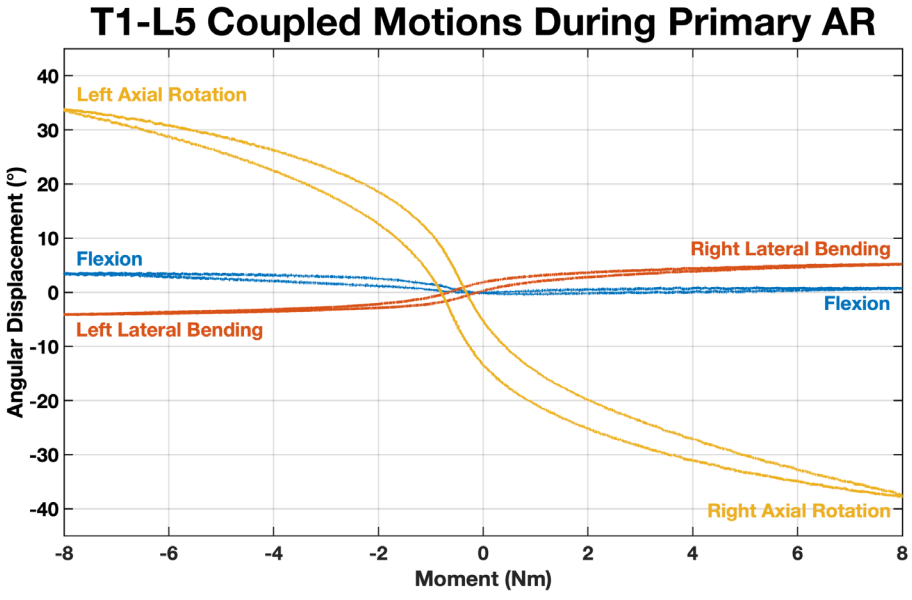

FIGURE 3 Exemplar moment–angular displacement curves of whole thoracic and lumbar (T1–L5) spinal coupled motions during primary flexion-extension (FE), lateral bending (LB), and axial rotation (AR) obtained from specimen 3 during the third unloading/loading cycle of pure, unconstrained bending moments of ±8 Nm.

consistent coupled FE pattern in the TS, but there was statistically significant ($p < 0.05$) coupled flexion in the LS.

4 | DISCUSSION

4.1 | Coupled motion patterns of the TS, TLJ, and LS

To the authors' knowledge, this is the first in vitro study to quantify the coupled motions of the whole human TS and LS (T1–L5) with rib cage. [TS] Several previous in vitro and in vivo studies concur with the current findings. Liebsch et al.,[10] under similar in vitro testing conditions, found no statistically significant TS-coupled motion patterns during primary FE. That study also reported general coupled extension and ipsilateral AR during primary LB in addition to an inconsistent pattern of coupled FE during primary AR. Ipsilateral coupled AR during primary LB was also reported in vivo; however, most of the TS underwent flexion.[38] Ipsilateral coupled LB during primary AR was also previously reported in vivo.[39,40] However, there are few contrasting reports in the literature. Contralateral coupled AR during primary LB in upper thoracic, four-vertebra specimens with rib cages,[15] and contralateral coupled LB primary AR[10] were reported in vitro.

[TLJ] In agreement with the current results, inconsistent TLJ-coupled motion patterns during primary FE have been reported both in vitro[17] and in vivo.[41] During primary LB, no consistent coupled FE and a general contralateral pattern of coupled AR were reported in vitro[17] and in vivo,[42] respectively. During primary AR, contralateral coupled LB was reported in vivo.[39] However, some studies do not concur with the current findings. During primary LB, while no consistent coupled AR[17] was observed in vitro, a trend of coupled extension[38,41] and an ipsilateral pattern of coupled AR[38] were observed in vivo. During primary AR, a trend of coupled flexion was reported both in vitro[17] and in vivo,[39,41] and an ipsilateral coupled LB pattern was reported in vitro.[17]

[LS] In agreement with the current findings, previous in vitro studies have reported inconsistent LS-coupled motion patterns[11,12] during primary FE. The contralateral relationship between LB and AR in the LS was also previously reported in vitro[11-13] and in vivo.[43,44] Coupled flexion during both primary LB and primary AR has also been reported in previous in vitro studies.[11-13] Contrastingly, consistent coupled extension during primary LB, and an inconsistent pattern of coupled FE during primary AR were reported in vivo.[43]

In general, it is difficult to directly compare results from in vitro and in vivo studies due to differences in loading, anatomical constraints, and boundary conditions. While in vivo studies offer the advantage of intact anatomical structures in their in situ loading environment, they are challenged by limited measurement modalities[42] and variance in participant age, anthropometry, personal comfort, and sagittal posture. Although not directly clinically relevant, in vitro studies offer the ability to controllably preposition the spine and apply known loads to measure kinematics, as well as to isolate the effects of structural and osteoligamentous factors without neuromuscular contributions.

4.2 | Coupled motion etiology

The bending mechanics of a C-shaped, circular rod of uniform cross-section (C-rod) can help explain spinal coupled motions. Intuitively, bending in the plane of the C-rod's curvature would solely cause in-plane primary FE without coupled LB or AR motions. In the current study, the inconsistent coupled motions observed during primary FE may be explained by slight coronal spinal curvatures, transverse plane spinal pre-rotation,[45,46] and deviations of vertebral alignment within the potting fixtures. With the concavity of the C-rod facing forward (i.e., a kyphotic curve) and the bottom end held fixed, an LB moment applied to the top of the C-rod will result in ipsilateral bending (i.e., the primary motion) with a concomitant ipsilateral AR (i.e., the coupled motion). On the other hand, with the convexity of the C-rod facing forward (i.e., a lordotic curve) and the bottom end held fixed, an LB moment applied to the top of the C-rod will result in ipsilateral bending with a concomitant contralateral AR. The aforementioned phenomena can help explain the observed ipsilateral thoracic and contralateral lumbar coupling between LB and AR.

Similarly, the human spine can be considered a rod that is S-shaped and segmented with non-uniform cross-section and varying anatomical constraints (i.e., intervertebral discs, facet joints, and spinal ligaments) that are symmetric only about the mid-sagittal plane. For these reasons, we theorize that significant coupled motions will only consistently occur in the normative human spine during primary LB and AR in the coronal and transverse planes, respectively, but not during primary FE in the mid-sagittal plane. Furthermore, we speculate that the thoracic extension and lumbar flexion tendencies observed during primary LB cause compression of the posterior thoracic vertebral structures and unloading of the posterior lumbar vertebral structures that further promote ipsilateral and contralateral coupled AR in the TS and LS, respectively. Similar speculation can be made for the coupled lumbar flexion observed during primary AR.

As the 6DOF spine motion simulator applied an unconstrained pure moment, slight coronal spinal curvatures, the slight pre-rotated structure of the spine in the transverse plane,[45,46] and deviations of vertebral alignment within the potting fixtures may have induced the unexpected, inconsistent coupled motion patterns that were observed during primary FE as well as the asymmetric coupled magnitudes that occurred during primary LB and AR (i.e., the statistically significant coupled motions during only one direction of primary LB and AR). It was expected for such motions to be statistically significant in both directions because of the anatomical symmetry of the spine across the midsagittal plane. Therefore, it is expected that future work with larger sample sizes will identify the consistent coupled motion patterns reported herein to be statistically significant in both directions of primary LB and AR. In addition, the variance in coupled motion patterns may be attributed to differences between specimens related to

vertebral body and disc morphology, as well as facet joint asymmetry.[31]

4.3 | Evaluation and influence of sagittal posture

The initial sagittal posture has been reported to influence the magnitude and pattern of observed coupled motions of the TS[31] and LS.[13] All specimens in this study exhibited thoracic kyphosis within the normal range of 10–40°,[47] except for specimens 2 and 6 which had slightly hyperkyphotic TSs with angles of 40.7° and 41.8°, respectively. Considering that the incidence of hyperkyphosis above 60 years of age is 20–40%,[48] such angles are not unexpected for these specimens. The lumbar lordosis angles for all specimens (19.4–27.2°) were within the normal range of 18–69°.[49] Notably, there were no visible or statistically significant correlations with thoracic kyphosis or lumbar lordosis angles and any of the coupled ROM values, a finding consistent with the observation made by Liebsch et al.[10] in the TS.

4.4 | Intra- and inter-regional differences in coupled LB and AR ROMs

After discovering a statistically significant coupling relationship between LB and AR, Wilcoxon signed-rank tests were performed to determine if one coupled motion was more prominent (i.e., had a greater ROM) than the other and if there were differences in these coupled ROMs between the TS and LS. No statistically significant differences in magnitude were found between the coupled LB and AR ROMs in any of the three spinal regions analyzed. Additionally, there were no significant differences in coupled LB or AR ROMs between the TS and LS.

4.5 | Limitations

The constraint offered by the rib cage on thoracic ROM has been previously reported.[15,50-52] While resecting a portion of the most cephalad rib necks to test some specimens may have slightly increased thoracic ROM at the corresponding level, there is no consensus on the effect of rib resection on in vitro coupling between LB and AR in the TS.[15,52] Additionally, the specimens from older donors used in this study were osteopenic based on their *T*-scores and may have had age-related disc degeneration that could have influenced spinal kinematics. While such effects can be reduced by using younger cadaveric specimens, there is a dearth of such samples. Nonetheless, the specimens used had an age range comparable to previous studies[15,53,54] and satisfied the previously mentioned radiographic screening for kinematics testing. Furthermore, due to the limited sample size, the results of this study may not capture the greater diversity in sex, age, spinal curvature, and disc degeneration observed in the human population which likely affect spine biomechanics. Future work with larger sample sizes may help quantify age- as well as sex-specific differences in coupled motion magnitudes within the TS and LS that result from related variations in vertebral morphology.[55-58] The methods used herein may also be applied to quantify the altered coupled motions of pathologic cadaveric spine specimens to better understand spinal instability resulting from altered biomechanics.

Intuitively, the results of this study lack the direct clinical utility possessed by results of in vivo studies that are influenced by the presence of other anatomical structures[59] as well as the neuromuscular system, a significant contributing factor to spinal coupled motion.[43] To better simulate physiological loading conditions, some previous in vitro studies have applied compressive preload or follower load during testing.[10,53,54,60–64] Although such loading conditions were not employed in the current test setup, the results of the present study provide insight into coupled motion behavior resulting from the postural and intrinsic mechanical properties of the spine in response to solely a pure moment, unaffected by the addition of other loads. Due to the complexity of applying preloads, especially when including the ribcage where standard preloading methods cannot be used,[10,53] solely pure moment-based testing may provide better standardization for comparing spinal kinematics data across in vitro studies. Overall, however, without recapitulating muscle forces or true in situ motion patterns, the results from in vitro studies lack the direct clinical relevance possessed by those from in vivo studies. Finally, due to differences in experimental design factors such as tissue preparation, test setup, amount of applied load, and measurement modalities, only the directionality of the coupled motion patterns observed herein could be compared with that of previous studies. Such methodological variability may partly contribute to conflicting coupled motion patterns reported previously.[14]

5 | CONCLUSIONS

The findings of this study support evidence of consistent mechanical coupled motion patterns during primary LB and AR in the TS and LS. The region-specific coupled motion patterns and magnitudes reported herein could serve as reference for validating high-fidelity computational models of the spine and assessing the influence of spinal deformities, implants, and experimental surgical techniques on kinematic characteristics of the TS and LS in future in vitro studies.

AUTHOR CONTRIBUTIONS

All the authors have made substantial contributions. Mattan R. Orbach conceived the study design, performed data and statistical analysis, and drafted the manuscript. Brandon S. Bucklen and Jonathan Mahoney provided the specimens, and Mattan R. Orbach and Jonathan Mahoney conducted the testing and acquired the data. Mattan R. Orbach and Sriram Balasubramanian performed data interpretation, designed the presentation methods, and critically revised the manuscript for important intellectual content with input from Jonathan Mahoney and Brandon S. Bucklen. Jonathan Mahoney and Brandon S. Bucklen also supervised the study and provided administrative support. All the authors read and approved the contents in the manuscript and agree to be accountable for its accuracy and integrity.

ACKNOWLEDGMENTS

The authors would like to thank Globus Medical, Inc. for providing the facilities and funding support to procure and test the cadaveric specimens.

CONFLICT OF INTEREST STATEMENT

The authors disclose that this study was performed at Globus Medical, Inc. (GMI), using its six-degrees-of-freedom motion simulator. MRO and SB have no disclosures to report. Cadaveric specimens and related materials were provided by GMI, at which JM and BSB are salaried employees with stock options.

ORCID

Mattan R. Orbach https://orcid.org/0000-0002-5178-7742
Sriram Balasubramanian https://orcid.org/0000-0002-7886-6184

REFERENCES

1. Lovett RW. The mechanism of the normal spine and its relation to scoliosis. *Bost Med Surg J*. 1905;*CLIII*:349-358.
2. White AA, Panjabi MM. *Clinical Biomechanics of the Spine*. 2nd ed. Lippincott Williams & Wilkins; 1990.
3. Veldhuizen AG, Scholten PJ. Kinematics of the scoliotic spine as related to the normal spine. *Spine*. 1987;*12*(9):852-858.
4. Beuerlein MJ, Raso VJ, Hill DL, Moreau MJ, Mahood JK. Changes in alignment of the scoliotic spine in response to lateral bending. *Spine*. 2003;*28*(7):693-698.
5. Panjabi MM, Oda T, Crisco JJ 3rd, Dvorak J, Grob D. Posture affects motion coupling patterns of the upper cervical spine. *J Orthop Res*. 1993;*11*(4):525-536.
6. Pearcy M, Portek I, Shepherd J. The effect of low-back pain on lumbar spinal movements measured by three-dimensional X-ray analysis. *Spine*. 1985;*10*(2):150-153.
7. Hindle RJ, Pearcy MJ, Cross AT, Miller DH. Three-dimensional kinematics of the human back. *Clin Biomech*. 1990;*5*(4):218-228.
8. Schultz AB, Belytschko TB, Andriacchi TP, Galante JO. Analog studies of forces in the human spine: mechanical properties and motion segment behavior. *J Biomech*. 1973;*6*(4):373-383.
9. Scholten PJ, Veldhuizen AG. The influence of spine geometry on the coupling between lateral bending and axial rotation. *Eng Med*. 1985;*14*(4):167-171.
10. Liebsch C, Graf N, Wilke HJ. The effect of follower load on the intersegmental coupled motion characteristics of the human thoracic spine: an in vitro study using entire rib cage specimens. *J Biomech*. 2018;*78*:36-44.
11. Cholewicki J, Crisco JJ 3rd, Oxland TR, Yamamoto I, Panjabi MM. Effects of posture and structure on three-dimensional coupled rotations in the lumbar spine. A biomechanical analysis. *Spine*. 1996;*21*(21):2421-2428.
12. Panjabi MM, Oxland TR, Yamamoto I, Crisco JJ. Mechanical behavior of the human lumbar and lumbosacral spine as shown by three-dimensional load-displacement curves. *J Bone Joint Surg Am*. 1994;*76*(3):413-424.
13. Panjabi M, Yamamoto I, Oxland T, Crisco J. How does posture affect coupling in the lumbar spine? *Spine*. 1989;*14*(9):1002-1011.
14. Sizer PS Jr, Brismée JM, Cook C. Coupling behavior of the thoracic spine: a systematic review of the literature. *J Manipulative Physiol Ther*. 2007;*30*(5):390-399.
15. Brasiliense LB, Lazaro BC, Reyes PM, Dogan S, Theodore N, Crawford NR. Biomechanical contribution of the rib cage to thoracic stability. *Spine*. 2011;*36*(26):E1686-E1693.
16. Mannen EM, Anderson JT, Arnold PM, Friis EA. Mechanical analysis of the human cadaveric thoracic spine with intact rib cage. *J Biomech*. 2015;*48*(10):2060-2066.
17. Oxland TR, Lin RM, Panjabi MM. Three-dimensional mechanical properties of the thoracolumbar junction. *J Orthop Res*. 1992;*10*(4):573-580.
18. Balasubramanian S, D'Andrea CR, Viraraghavan G, Cahill PJ. Development of a finite element model of the pediatric thoracic and lumbar spine, ribcage, and pelvis with orthotropic region-specific vertebral growth. *J Biomech Eng*. 2022;*144*(10):101007.
19. D'Andrea CR, Samdani AF, Balasubramanian S. Patient-specific finite element modeling of scoliotic curve progression using region-specific stress-modulated vertebral growth. *Spine Deform*. 2023;*11*(3):525-534.
20. Hadagali P, Peters JR, Balasubramanian S. Morphing the feature-based multi-blocks of normative/healthy vertebral geometries to scoliosis vertebral geometries: development of personalized finite element models. *Comput Methods Biomech Biomed Engin*. 2018;*21*(4):297-324.
21. Alfraihat A, Samdani AF, Balasubramanian S. Predicting curve progression for adolescent idiopathic scoliosis using random forest model. *PLoS One*. 2022;*17*(8):e0273002.
22. Harris JA, Mayer OH, Shah SA, Campbell RM Jr, Balasubramanian S. A comprehensive review of thoracic deformity parameters in scoliosis. *Eur Spine J*. 2014;*23*(12):2594-2602.
23. Alfraihat A, Olson JC, Snyder BD, Cahill PJ, Balasubramanian S. Thoracic vertebral morphology in normal and scoliosis deformity in skeletally immature rabbits: a longitudinal study. *JOR Spine*. 2020;*3*(4):e1118.
24. Lopez-Valdes FJ, Riley PO, Lessley DJ, et al. The six degrees of freedom motion of the human head, spine, and pelvis in a frontal impact. *Traffic Inj Prev*. 2014;*15*(3):294-301.
25. Mathews EA, Balasubramanian S, Seacrist T, et al. Comparison of pediatric and young adult far-side head kinematics in low-speed lateral and oblique impacts. Paper presented at 23rd International Technical Conference on the Enhanced Safety of Vehicles (ESV) National Highway Traffic Safety Administration; 2013.
26. Seacrist T, Arbogast KB, Maltese MR, et al. Kinetics of the cervical spine in pediatric and adult volunteers during low speed frontal impacts. *J Biomech*. 2012;*45*(1):99-106.
27. Lopez-Valdes F, Seacrist T, Balasubramanian S, et al. Comparing the kinematics of the head and spine between volunteers and PMHS: a methodology to estimate the kinematics of pediatric occupants in a frontal impact. Paper presented at Proceedings of International Research Conference on the Biomechanics of Impact; 2011.
28. Arbogast KB, Balasubramanian S, Seacrist T, et al. Comparison of kinematic responses of the head and spine for children and adults in low-speed frontal sled tests. *Stapp Car Crash J*. 2009;*53*:329-372.
29. Balasubramanian S, Peters JR, Robinson LF, Singh A, Kent RW. Thoracic spine morphology of a pseudo-biped animal model (kangaroo) and comparisons with human and quadruped animals. *Eur Spine J*. 2016;*25*(12):4140-4154.
30. Panjabi MM. Biomechanical evaluation of spinal fixation devices: I. A conceptual framework. *Spine*. 1988;*13*(10):1129-1134.
31. Edmondston SJ, Aggerholm M, Elfving S, et al. Influence of posture on the range of axial rotation and coupled lateral flexion of the thoracic spine. *J Manipulative Physiol Ther*. 2007;*30*(3):193-199.
32. Borkowski SL, Tamrazian E, Bowen RE, Scaduto AA, Ebramzadeh E, Sangiorgio SN. Challenging the conventional standard for thoracic spine range of motion: a systematic review. *JBJS Rev*. 2016;*4*(4):e51-e511.
33. Goel VK, Panjabi MM, Patwardhan AG, Dooris AP, Serhan H. Test protocols for evaluation of spinal implants. *J Bone Joint Surg Am*. 2006;*88*(Suppl 2):103-109.
34. Wilke HJ, Herkommer A, Werner K, Liebsch C. In vitro analysis of the segmental flexibility of the thoracic spine. *PLoS One*. 2017;*12*(5):e0177823.

35. Wilke HJ, Jungkunz B, Wenger K, Claes LE. Spinal segment range of motion as a function of in vitro test conditions: effects of exposure period, accumulated cycles, angular-deformation rate, and moisture condition. *Anat Rec*. 1998;*251*(1):15-19.
36. Schmidt J, Berg DR, Ploeg H, Ploeg L. Precision, repeatability and accuracy of Optotrak® optical motion tracking systems. *Int J Exp Comput Biomech*. 2009;*1*(1):114.
37. Maletsky LP, Sun J, Morton NA. Accuracy of an optical active-marker system to track the relative motion of rigid bodies. *J Biomech*. 2007;*40*(3):682-685.
38. Fujimori T, Iwasaki M, Nagamoto Y, et al. Kinematics of the thoracic spine in trunk lateral bending: in vivo three-dimensional analysis. *Spine J*. 2014;*14*(9):1991-1999.
39. Fujimori T, Iwasaki M, Nagamoto Y, et al. Kinematics of the thoracic spine in trunk rotation: in vivo 3-dimensional analysis. *Spine*. 2012;*37*(21):E1318-E1328.
40. Willems JM, Jull GA, J KF. An in vivo study of the primary and coupled rotations of the thoracic spine. *Clin Biomech*. 1996;*11*(6):311-316.
41. Gercek E, Hartmann F, Kuhn S, Degreif J, Rommens PM, Rudig L. Dynamic angular three-dimensional measurement of multisegmental thoracolumbar motion in vivo. *Spine*. 2008;*33*(21):2326-2333.
42. Gregersen GG, Lucas DB. An in vivo study of the axial rotation of the human thoracolumbar spine. *J Bone Joint Surg Am*. 1967;*49*(2):247-262.
43. Pearcy MJ, Tibrewal SB. Axial rotation and lateral bending in the normal lumbar spine measured by three-dimensional radiography. *Spine*. 1984;*9*(6):582-587.
44. Miles M, Sullivan WE. Lateral bending at the lumbar and lumbosacral joints. *Anat Rec*. 1961;*139*(3):387-398.
45. Kouwenhoven JW, Vincken KL, Bartels LW, Castelein RM. Analysis of preexistent vertebral rotation in the normal spine. *Spine*. 2006;*31*(13):1467-1472.
46. Kouwenhoven JW, Bartels LW, Vincken KL, et al. The relation between organ anatomy and pre-existent vertebral rotation in the normal spine: magnetic resonance imaging study in humans with situs inversus totalis. *Spine*. 2007;*32*(10):1123-1128.
47. O'Brien MF, Kuklo TR, Blanke KM, Lenke LG. *Spinal Deformity Study Group Radiographic Measurement Manual*. Medtronic Sofamor Danek USA, Inc.; 2008.
48. Zappalá M, Lightbourne S, Heneghan NR. The relationship between thoracic kyphosis and age, and normative values across age groups: a systematic review of healthy adults. *J Orthop Surg Res*. 2021;*16*(1):447.
49. Stagnara P, De Mauroy JC, Dran G, et al. Reciprocal angulation of vertebral bodies in a sagittal plane: approach to references for the evaluation of kyphosis and lordosis. *Spine*. 1982;*7*(4):335-342.
50. Watkins R, Watkins R 3rd, Williams L, et al. Stability provided by the sternum and rib cage in the thoracic spine. *Spine*. 2005;*30*(11):1283-1286.
51. Liebsch C, Wilke HJ. Rib presence, anterior rib cage integrity, and segmental length affect the stability of the human thoracic spine: an in vitro study. *Front Bioeng Biotechnol*. 2020;*8*:46.
52. Mannen EM, Anderson JT, Arnold PM, Friis EA. Mechanical contribution of the rib cage in the human cadaveric thoracic spine. *Spine*. 2015;*40*(13):E760-E766.
53. Sis HL, Mannen EM, Wong BM, et al. Effect of follower load on motion and stiffness of the human thoracic spine with intact rib cage. *J Biomech*. 2016;*49*(14):3252-3259.
54. Anderson DE, Mannen EM, Tromp R, et al. The rib cage reduces intervertebral disc pressures in cadaveric thoracic spines by sharing loading under applied dynamic moments. *J Biomech*. 2018;*70*:262-266.
55. Peters JR, Servaes SE, Cahill PJ, Balasubramanian S. Morphology and growth of the pediatric lumbar vertebrae. *Spine J*. 2021;*21*(4):682-697.
56. Peters JR, Campbell RM Jr, Balasubramanian S. Characterization of the age-dependent shape of the pediatric thoracic spine and vertebrae using generalized procrustes analysis. *J Biomech*. 2017;*63*:32-40.
57. Peters JR, Chandrasekaran C, Robinson LF, Servaes SE, Campbell RM Jr, Balasubramanian S. Age-and gender-related changes in pediatric thoracic vertebral morphology. *Spine J*. 2015;*15*(5):1000-1020.
58. Seacrist T, Saffioti J, Balasubramanian S, et al. Passive cervical spine flexion: the effect of age and gender. *Clin Biomech*. 2012;*27*(4):326-333.
59. Orbach MR, Servaes SE, Mayer OH, Cahill PJ, Balasubramanian S. Quantifying lung and diaphragm morphology using radiographs in normative pediatric subjects, and predicting CT-derived lung volume. *Pediatr Pulmonol*. 2021;*56*(7):2177-2185.
60. Rohlmann A, Neller S, Claes L, Bergmann G, Wilke HJ. Influence of a follower load on intradiscal pressure and intersegmental rotation of the lumbar spine. *Spine*. 2001;*26*(24):E557-E561.
61. Wilke HJ, Rohlmann A, Neller S, Graichen F, Claes L, Bergmann G. ISSLS prize winner: a novel approach to determine trunk muscle forces during flexion and extension: a comparison of data from an in vitro experiment and in vivo measurements. *Spine*. 2003;*28*(23):2585-2593.
62. Fry RW, Alamin TF, Voronov LI, et al. Compressive preload reduces segmental flexion instability after progressive destabilization of the lumbar spine. *Spine*. 2014;*39*(2):E74-E81.
63. Stanley SK, Ghanayem AJ, Voronov LI, et al. Flexion-extension response of the thoracolumbar spine under compressive follower preload. *Spine*. 2004;*29*(22):E510-E514.
64. Patwardhan AG, Havey RM, Meade KP, Lee B, Dunlap B. A follower load increases the load-carrying capacity of the lumbar spine in compression. *Spine*. 1999;*24*(10):1003-1009.

How to cite this article: Orbach, M. R., Mahoney, J., Bucklen, B. S., & Balasubramanian, S. (2023). In vitro coupled motions of the whole human thoracic and lumbar spine with rib cage. *JOR Spine*, *6*(3), e1257. https://doi.org/10.1002/jsp2.1257

APPENDIX A

TABLE A1 Median, first quartile (Q1), and third quartile (Q3) values of thoracic (T1–T12, $n = 5$), thoracolumbar junction (T12–L1, $n = 7$), and lumbar (L1–L5, $n = 7$) coupled motions occurring during the positive and negative directions of each primary motion. Flexion, right lateral bending, and left axial rotation are in the positive direction. Extension, left lateral bending, and right axial rotation are in the negative direction.

			Primary FE (°)			Primary LB (°)			Primary AR (°)		
			Median	Q1	Q3	Median	Q1	Q3	Median	Q1	Q3
Thoracic (T1–T12)	Primary motion (+)	FE	16.6	15.4	18.8	−1.0	−1.6	−0.8	6.6	5.1	10.0
		LB	−0.3	−0.8	1.0	16.8	15.3	17.5	−6.9	−8.2	−3.4
		AR	−3.0	−5.6	2.3	−3.1	−5.3	2.4	27.8	26.9	31.7
	Primary motion (−)	FE	−17.5	−18.9	−16.7	−0.7	−2.3	1.2	−2.5	−5.5	−2.3
		LB	−2.1	−2.4	1.8	−18.0	−18.0	−16.6	11.1	8.7	12.3
		AR	3.4	−2.1	4.5	4.4	2.7	5.1	−31.4	−33.9	−29.0
Thoracolumbar junction (T12–L1)	Primary motion (+)	FE	1.3	1.0	1.9	−0.8	−1.2	−0.3	−0.8	−2.6	−0.5
		LB	−0.6	−0.7	0.2	1.3	1.2	1.8	−0.2	−0.5	0.4
		AR	−0.6	−1.0	1.6	0.5	−0.2	0.6	1.0	0.6	7.1
	Primary motion (−)	FE	−1.0	−1.3	−0.6	0.4	−0.1	0.5	1.3	0.8	1.6
		LB	0.8	0.4	1.3	−1.0	−1.2	−0.7	−0.6	−0.9	−0.5
		AR	0.9	−0.1	1.6	−0.5	−0.6	0.2	−0.7	−1.4	0.3
Lumbar (L1–L5)	Primary motion (+)	FE	10.2	8.5	13.6	3.2	0.7	3.5	1.2	−1.1	2.4
		LB	−1.2	−2.3	1.2	10.3	8.0	11.7	1.4	0.3	1.9
		AR	1.8	−0.3	2.8	2.2	−1.1	4.0	10.3	9.4	10.9
	Primary motion (−)	FE	−9.8	−10.0	−7.3	1.1	−2.2	1.6	2.5	1.8	3.6
		LB	−1.1	−1.8	0.2	−12.7	−12.9	−11.1	−3.7	−4.2	−3.0
		AR	−2.5	−3.4	−1.5	−2.4	−4.8	−0.5	−11.8	−12.8	−10.5

Abbreviations: AR, axial rotation; FE, flexion-extension; LB, lateral bending.